A laser-cutting-based manufacturing process for the generation of three-dimensional scaffolds for tissue engineering using Polycaprolactone/Hydroxyapatite composite polymer

Jakob Schmid[1,2,3], Sascha Schwarz[1,4], Martina Fischer[3], Stefanie Sudhop[1,5], Hauke Clausen-Schaumann[1,5], Matthias Schieker[2] and Robert Huber[1,3]

Abstract

A manufacturing process for sheet-based stacked scaffolds (SSCs) based on laser-cutting (LC) was developed. The sheets consist of Polycaprolactone/Hydroxyapatite (PCL/HA) composite material. Single sheets were cut from a PCL/HA foil and stacked to scaffolds with interconnecting pores of defined sizes. HA quantities up to 50% were processable with high reproducibility, while the accuracy was dependent on the applied laser power. The smallest achievable pore sizes were about 40 μm, while the smallest stable solid structures were about 125 μm. The human mesenchymal stem cell line SCP-1 was cultured on the manufactured PCL/HA scaffolds. The cells developed a natural morphology and were able to differentiate to functional osteoblasts. The generation of PCL/HA SSCs via LC offers new possibilities for tissue engineering (TE) approaches. It is reliable and fast, with high resolution. The SSC approach allows for facile cell seeding and analysis of cell fate within the three-dimensional cell culture, thus allowing for the generation of functional tissue constructs.

Introduction

Scaffolds are commonly used in bone tissue engineering (TE) as a support for cell adhesion and to guide three-dimensional (3D) growth.[1] To generate functional tissue equivalents, the scaffolds should provide a suitable pore size, porosity, and an interconnecting pore structure.[2,3] Furthermore, biocompatibility, resorbability, and osteoinductivity are important for successful bone TE approaches.[4–6]

In general, these requirements are met by natural scaffolds such as decellularized bone grafts (e.g. from bovine femur spongiosa). However, these materials inherit the potential of pathogen transfer and immune rejection, as well as high variation in pore size and porosity.[7,8]

Consequently, in recent years, synthetic materials have been investigated and evaluated in their potential

[1]Center for Applied Tissue Engineering and Regenerative Medicine (CANTER), University of Applied Sciences Munich, Munich, Germany
[2]Laboratory of Experimental Surgery and Regenerative Medicine (ExperiMed), Ludwig-Maximilians University Munich, Munich, Germany
[3]Department of Industrial Engineering and Management, University of Applied Sciences Munich, Munich, Germany
[4]Department of Mechanical Engineering, Technical University of Munich, Garching, Germany
[5]Center for Nanoscience (CeNS), Ludwig Maximilian University of Munich, Munich, Germany

Corresponding author:
Robert Huber, Center for Applied Tissue Engineering and Regenerative Medicine (CANTER), University of Applied Sciences Munich, Lothstr. 34, 80335 Munich, Germany.
Email: robert.huber@hm.edu

to replace natural scaffolds, to provide equally potent matrices for cell adhesion, growth, and differentiation. Synthetic thermoplastic polymers like Polycaprolactone (PCL), Polylactide (PLA), Polyglycolide (PGA), or their corresponding copolymers show suitable properties for the generation of scaffolds for bone TE. Besides being biocompatible, resorbable, and Food and Drug Administration (FDA)-approved, PCL has been shown to be both osteoconductive and osteoinductive, which is both mandatory to ensure cell growth and differentiation on the scaffold. Furthermore, PCL is soluble in common organic solvents, which makes it accessible for rapid prototyping manufacturing techniques.[4,5,9,10]

To further improve the properties of PCL, composite materials can be created by adding bioactive materials, for instance, bioceramics, to the polymer. A broadly used bioceramic material for creating PCL-based composite materials is hydroxyapatite (HA, $Ca_{10}(PO_4)_6(OH)_2$), since it is of the same chemical composition as the inorganic phase of natural bone.[4,9,11]

The use of a PCL/HA composite material results in enhanced osteoconductivity and osteoinductivity, as well as in improved mechanical properties compared to PCL only. Furthermore, alkaline metabolic waste products are released during the resorption of HA. These can effectively neutralize acidic metabolic waste products, which occur during natural hydrolysis of PCL. Thus, critically low pH values can be avoided in degrading PCL/HA-based implants.[4,12] These characteristics make PCL/HA composite materials a promising material for the generation of scaffolds for bone TE.

For bone TE applications, most scaffolds are designed as solid structures, since these are beneficial for mimicking the mechanical properties of bone and retaining the desired geometry.[4,5,13] However, achieving spatially uniform cell distributions after cell seeding is difficult in solid scaffolds. Therefore, dynamic cell seeding procedures have to be developed, which have to be optimized for each scaffold design individually.[14–16] In addition, the investigation of cell fate in a solid 3D-cell culture (3DCC) can only be performed by cutting or sawing the tissue-engineered construct (TEC). As a consequence, the TEC cannot be used for further applications.

A sheet-based scaffold concept offers a solution to these drawbacks of scaffold-based TE. Hereby, single sheets are manufactured and stacked to form a 3D scaffold (referred to as stacked scaffold, SSC).[6,17] The advantages of SSCs are that single sheets can be seeded with cells individually and investigated with regard to cell distribution before the seeded sheets are stacked to an SSC. Moreover, cell distributions can be investigated after cultivation, by disassembling the SSC into single sheets. Furthermore, a sheet-based design can be used to combine both, solid structures and hydrogels for instance for vascularization approaches.[5,17]

Many manufacturing techniques—such as fused deposition modeling (FDM) and electrospinning—have been applied for the generation of scaffolds from PCL/HA composite materials.[6,9,18,19] With the help of those techniques, scaffolds can be created in a highly reproducible way, while pore size and porosity can be controlled to allow for cell ingrowth and migration as well as for nutrient supply during dynamic cultivation. However, the generation of PCL/HA sheets via FDM requires non-standard 3D printing devices and sophisticated techniques to obtain a printable mixture that remains stable after printing.[18,20] Furthermore, the process is prone to clogging of the printing nozzle due to HA particles. Bigger printing nozzles can prevent clogging, but only at the expense of printing resolution. Due to the relatively low melting temperature of PCL, the resolution can be further impaired by the heated nozzle. When a new layer is added to the printed construct, the heat of the nozzle can deform fine structure in subjacent layers.[21] In electrospinning, the pore size of the resulting scaffolds is not easily controllable and limited to smaller pore sizes. Therefore, electrospinning is not an option for applications where larger pore sizes and geometries are desired.[6,10,22,23] Techniques like porogen leaching are also limited to thin scaffold constructs since porogens have to be removed entirely from the generated scaffold, which is difficult especially for larger structures. Furthermore, interconnecting pore structures are hard to achieve in a controlled way.[22,24]

Laser-cutting (LC) is a manufacturing technique, which has not been investigated for the generation of sheet-based scaffolds so far. In LC devices, a continuous wave laser is used to process materials with very high precision.[25,26] Templates for the cutting process can be generated by computer-aided design (CAD). Thus, the manufacturing process is highly flexible with respect to the final design of a generated sheet and the resulting 3D scaffold.

Consequently, we developed a new manufacturing procedure based on LC, for the generation of PCL/HA sheets for 3DCC, which is shown in the present study. LC offers the possibility for a fast and reproducible generation of sheets and scaffolds. By using LC, certain drawbacks of common manufacturing techniques, like FDM or electrospinning, can be circumvented. Furthermore, the sheet-based scaffold approach enables for facile and easy cell seeding and investigation of cell growth and distribution.

Materials and methods

Generation of a PCL/HA foil

To produce a PCL/HA foil of 200 μm thickness, a 25×35 cm mold with a 200 μm recess was used. The mold was milled out of an aluminum block, to guarantee a fast removal of thermal energy after the cutting process, which is mandatory for the generation of fine structures. To generate the PCL/HA composite material, HA nanopowder (Sigma Aldrich) was dispersed in chloroform (Sigma Aldrich). Subsequently, PCL pellets (Sigma Aldrich) were
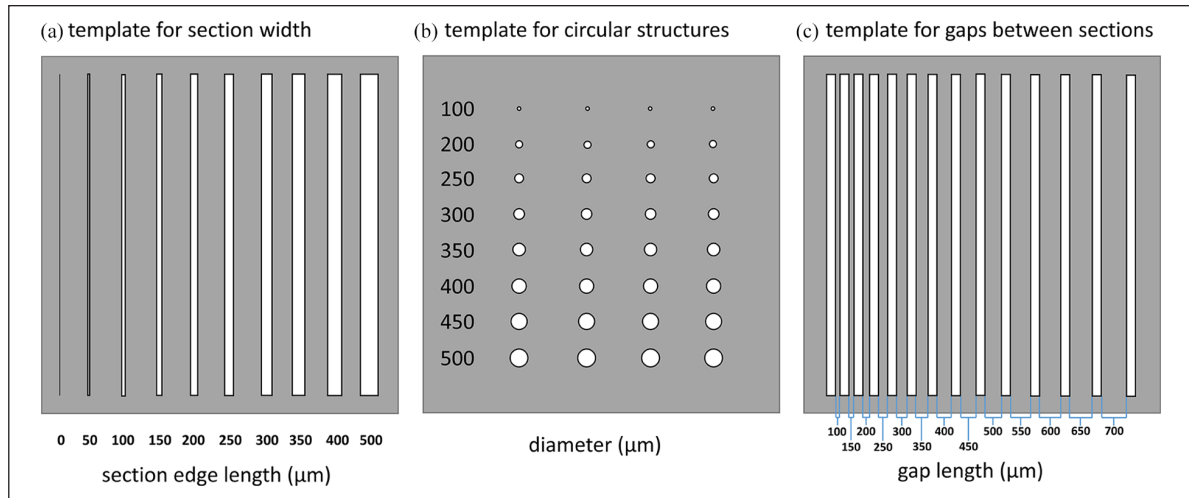
Figure 1. Test templates for the evaluation of the accuracy and the limits of the laser-cutting process: (a) test template for section width, varying from 0 to 500 µm (0 equals only a straight line, no rectangular shape in the designed template); (b) test template for circular structures with varying diameters from 100 to 500 µm; and (c) test template for gaps between sections, varying between 100 and 700 µm.

solubilized in the chloroform solution with continuous stirring. After the PCL pellets dissolved completely, the solution was heated to 60°C, until the slurry was highly viscous. The slurry was poured in the aluminum mold and heated to 80°C until the chloroform evaporated completely. Subsequently, the PCL/HA slurry was spread and smoothened in the mold using a pre-heated, round profile aluminum bar and cooled to RT prior to further processing via LC. The experiments conducted in this work were performed with a 75% PCL, 25% HA composite material.

Generation of PCL/HA sheets by LC

Adobe Illustrator CS6 (Adobe Systems) was used, to create cutting templates for the laser cutter. PCL/HA sheets were produced using a Zing 24 laser cutter (Epilog) equipped with a 30 W, continuous wave CO_2 laser. The PCL/HA foil was cut into 10×10 mm sheets at 6 W laser power (corresponding to 20%) and maximum laser head travel speed. Subsequently, the aluminum mold was cooled down to 4°C for easy removal of the sheets. Sheets were removed from the mold using a scalpel, sterilized in 80% EtOH for 20 minutes and stored at RT.

To evaluate the accuracy and limits of the cutting process, three different test templates were created and cut out of a 75% PCL, 25% HA (75PCL25HA) foil. For the generation of test templates, the width of cut sections (section width), the gap between cut sections (section gap), and the diameter of circular structures (circle diameter) were varied (Figure 1). To evaluate the effect of different applied laser power levels on the accuracy, the templates were cut at levels between 0.3 and 12 W (1%–40%). For each laser power level, five equal test templates were manufactured.

To investigate the robustness of the cutting process, the deviations between equal structures (e.g. the widths of cut sections) on the created sheets were measured using a Zeiss Axio Observer.Z1 (Carl Zeiss) equipped with a 2.5× objective and analyzed using the Zen V2.6 software (Carl Zeiss). Subsequently, mean values (MVs) and standard deviations (SDs) were calculated. To investigate the accuracy of the cutting process, deviations between the manufactured sheets and the corresponding templates were calculated. For each laser power value used, MVs and SDs were calculated from the determined deviations.

Mechanical properties of 75PCL25HA sheets

The ultimate tensile strength (UTS) and the Young's modulus (YM) of single 75PCL25HA sheets (geometry 2, see Figure 4) were measured using a Mach1 mechanical tester (Biomomentum) with a 75 N load cell. The mechanical properties were determined in a dry state using a head speed of 0.2 mm/second. MVs and SDs were calculated from the measurements.

Scanning electron microscopy and energy-dispersive X-ray spectroscopy

To investigate, if residual aluminum particles remain on the PCL/HA sheets after the LC process, scanning electron microscopy (SEM) and energy-dispersive X-ray spectroscopy (EDX) were performed. Therefore, manufactured sheets were sputter coated with platinum and subsequently analyzed using a Lyra 3 system (Tescan). Imaging was performed at 5 kV using a secondary electron detector and the associated LycaTC software (Tescan). EDX was performed

at 10 kV using an X-Max silicon drift detector (Oxford Instruments) and the associated Aztec software (Oxford Instruments).

Cell culture

The human mesenchymal stem cell (hMSC) line SCP-1, modified to express green fluorescent protein (GFP) constitutively,[27] was used for the experiments. Cells were cultured at 37°C using Dulbecco's Modified Eagle Medium (DMEM, Merck) with 200 mM Glutamax (Gibco), 100 U/mL Penicillin/Streptomycin (Biochrom), and 10% fetal bovine serum (FBS, Biochrom) in a humidified 90% air, 10% CO_2 atmosphere. Quadratic 75PCL25HA sheets with edge lengths of 10 mm and a grid of 19 rectangular sections with 300 μm section width were used for the experiments (see Figure 4(a)).

To analyze cell growth and distribution, 50,000 SCP-1 cells were seeded by pipetting 100 μL of a 5×10^5 cells/mL suspension on each sheet. Subsequently, the cells were cultivated statically for 5 days, while the medium was changed every 48 hours. Cells cultivated on unprocessed PCL/HA foil and on cell culture dishes were used as a control, to investigate if the processing of PCL/HA by LC affects cell adherence and growth, for example, by structural alterations of the polymer in the heat affected zone (HAZ) of the laser. GFP producing cells were analyzed at 475 nm using a Zeiss Axio Observer.Z1 (Carl Zeiss) microscope and the associated Zen V2.6 software (Carl Zeiss).

Cell differentiation

To investigate cellular responses to differentiation factors, SCP-1 cells growing on manufactured PCL/HA sheets were differentiated to osteoblasts using the StemPro Osteogenesis Differentiation Kit (Thermo Fisher). Cells were seeded on single 75PCL25HA sheets (see "Cell culture" section) and cultivated statically in DMEM until 60%–80% confluency was reached. Subsequently, the cells growing on the sheets were cultivated in osteogenic differentiation medium (ODM) for a minimum of 21 days. The medium was changed every 2 days to provide a sufficient nutrient supply. Cells growing on unprocessed PCL/HA and on cell culture dishes, as well as cells cultivated in DMEM were used as a control.

The differentiation of hMSCs to osteoblasts was verified by staining calcium depositions in the mineralized extracellular matrix of mature osteoblasts, using Alizarin-Red S staining (ARS, Merck). Therefore, single sheets were incubated in ARS for 2 minutes and subsequently rinsed with PBS solution (Merck). Overgrown sheets, which were cultivated in DMEM were used as a negative control. ARS stained sheets were analyzed at 405 nm, using a Zeiss Axio Observer.Z1 microscope and the associated Zen V2.6 software.

3D cell culture

For 3D cell culture, circular 75PCL25HA sheets with 10 mm diameter and a grid of 19 rectangular sections were used (see Figure 4(b)). Fifty sheets were seeded with 50,000 SCP-1 cells each, by pipetting 100 μL of a 5×10^5 cells/mL suspension on each sheet. After 1 hour of static incubation, sheets were stacked in an alternating way (consecutive sheets rotated by 90°), to form a scaffold with interconnecting pores (referred to as SSC) (Figure 2).

Subsequently, the SSC was placed in a perfusion microbioreactor system and cultivated dynamically for 5 days. During the cultivation, oxygen levels were controlled at 15% to guarantee sufficient oxygen and nutrient supply as described elsewhere.[28] To investigate cell growth and distribution and to investigate if the SSC offers a coherent structure with interconnecting pores, the SSC was taken out of the bioreactor and disassembled after the cultivation. Subsequently, the cells growing on the sheets were analyzed at 475 nm (GFP) using a Zeiss Axio Observer.Z1 microscope and the associated Zen V2.6 software.

Results

Generation of PCL/HA sheets

Sheets were generated from PCL/HA foil by LC. PCL/HA slurries with HA-quantities of up to 50% were suitable for the production process. When higher amounts of HA were used, slurries could not be smoothened sufficiently, resulting in a PCL/HA foil of insufficient quality for the subsequent LC; 25% HA slurries gave the best results with regard to processability and sheet stability. Consequently, sheets containing 75% PCL and 25% HA (75PCL25HA) were used for the subsequent experiments.

Laser powers below 3 W (10% of the maximum power) were not sufficient for cutting the PCL/HA foil and are thus not suitable for processing the PCL/HA foil. For laser power values between 3 and 12 W (10%–40%), the variation between cut structures was constantly ≤20 μm for all applied power settings. For laser powers above 3 W (10%), the removal of material during the LC process affected the accuracy of the procedure, with deviations between designed templates and resulting sheets increasing linearly with increasing laser power (Figure 3). Material removal led to both larger sections and diameters as well as thinner gaps between sections—except for 100 μm circular structures when cutting with 4.5 W laser power or lower, which resulted in smaller diameters.

Resulting structures, which were thinner than 125 μm, were not reliably stable. These structures were easily damaged during removal from the aluminum mold or removed entirely by the lasers' power input during the cutting process.

Using 6 W laser power (20% of maximum power) resulted in a well controllable process and was used for the production of 75PCL25HA sheets for all subsequent
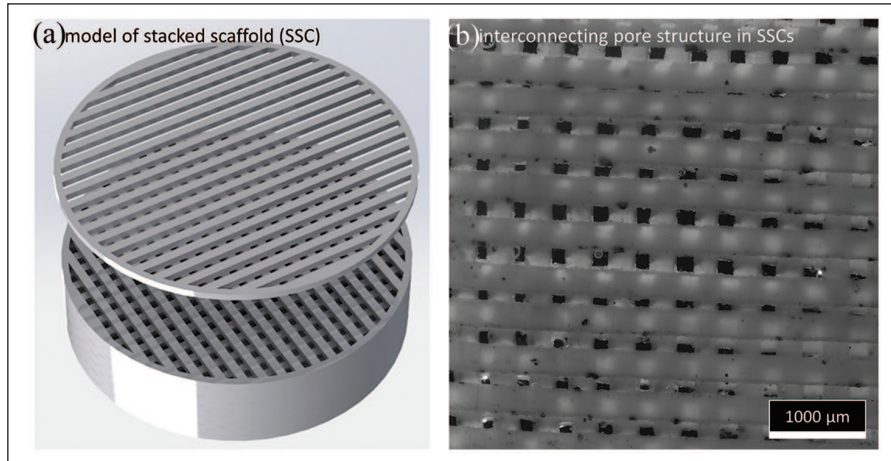
Figure 2. Model and structure of a stacked scaffold (SSC): (a) model of a stacked scaffold, illustrating the alternating way, how sheets are stacked and (b) resulting interconnecting pore structure of SSCs.
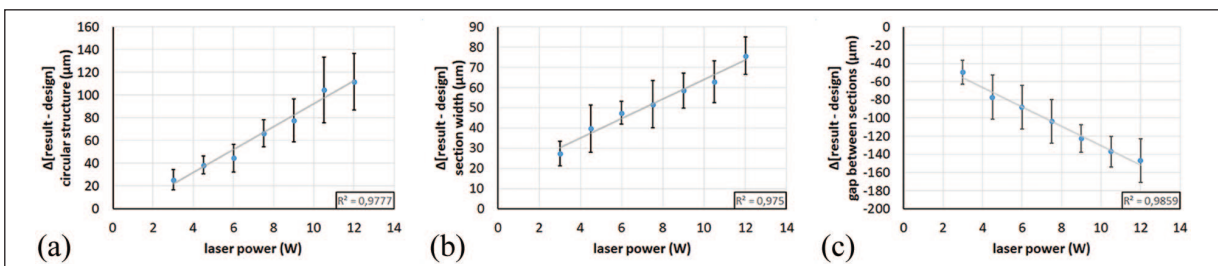

Figure 3. Evaluation of the cutting accuracy depending on the applied laser power for 75PCL25HA sheets: Mean values and standard deviations (MV $\pm$ SD, n = 5) calculated from differences between manufactured sheets and designed cutting templates: (a) deviations for diameters of circular structures, (b) deviations for section widths, and (c) deviations for gaps between sections.
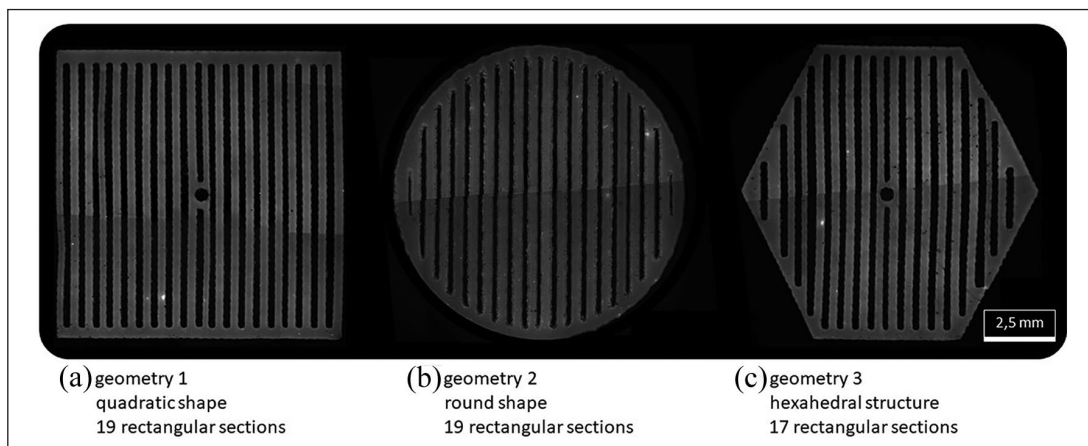

(a) geometry 1
quadratic shape
19 rectangular sections

(b) geometry 2
round shape
19 rectangular sections

(c) geometry 3
hexahedral structure
17 rectangular sections

Figure 4. Different geometries cut from 75PCL25HA foil at 6 W laser power: (a) quadratic shape (10 × 10 mm), 19 rectangular sections (9.5 mm × 0.3 mm), central circular section, for example, for sensor placement within the scaffold; (b) circular shape (10 mm diameter), 19 rectangular sections (varying length × 0.3 mm); and (c) hexahedral shape (10 × 10 mm), 17 rectangular sections (varying length × 0.3 mm), central circular section, for example, for sensor placement within the scaffold.

experiments. The cutting templates were adjusted to account for the determined deviation accordingly. To demonstrate the flexibility of the LC process, quadratic (geometry 1), circular (geometry 2), and hexahedral (geometry 3)

shaped sheets were cut from a 75PCL25HA foil (Figure 4). All geometries shared the same diameter of 10 mm with equally distributed sections. Section widths were designed to be 250 µm (resulting in section widths of approximately
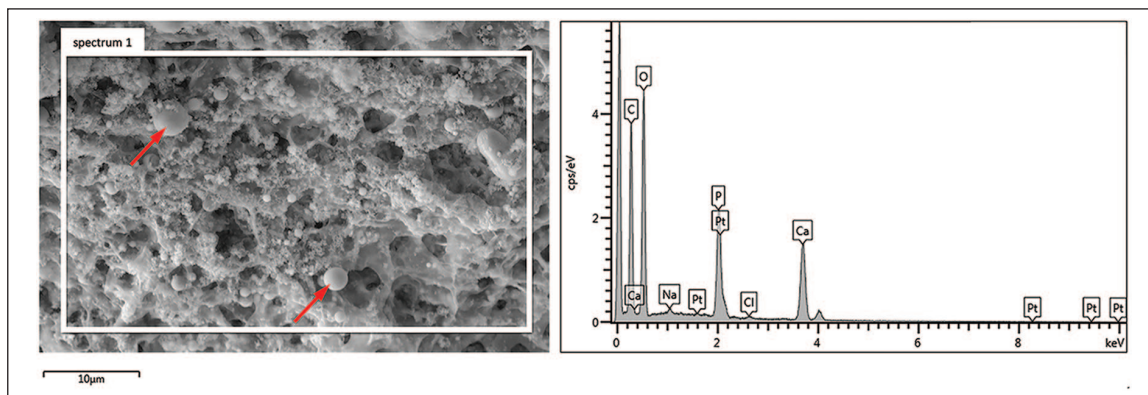
Figure 5. SEM image and EDX analysis of 75PCL25HA sheet.
SEM image and EDX analysis of the cut edge of a manufactured 75PCL25HA sheet. HA nanoparticles embedded in PCL are visible in the SEM image (2 nanoparticles are indicated exemplary by arrows). EDX analysis was performed in the area of the white box.

300 μm). A central circular hole was added in geometry 1 and 3, to accommodate for the insertion of a sensor into the scaffold, for instance, for pO_2 or pH measurements inside of the 3DCC. Using the developed manufacturing process, five sheets could be generated per minute, whereas the manufacturing speed varied slightly depending on the geometry.

Mechanical properties of 75PCL25HA sheets. The mechanical properties of 75PCL25HA sheets (geometry 2, see Figure 4) were determined using a Mach1 mechanical tester. To determine the YM and the UTS, the force-affected cross-section area was calculated from a CAD model while having regard to the deviations of the manufacturing process (Figure 3). The YM was determined at 110 ± 18 MPa, and the UTS at 3.05 ± 0.80 MPa (n = 5).

SEM and EDX. Since an aluminum mold is used in the manufacturing process of PCL/HA sheets, the sheets were examined by SEM and EDX, to investigate if residual aluminum particles remain on the manufactured sheets. Several surfaces, including cut edges, were imaged and examined. HA nanoparticles embedded in PCL were clearly visible in the SEM image. In the EDX analysis, the following elements were found: Carbon (C), oxygen (O), calcium (Ca), phosphorous (P), and platinum (Pt), which are the main components of PCL $((C_6H_{10}O_2)_n)$ and HA $(Ca_{10}(PO_4)_6(OH)_2)$. Furthermore, traces of sodium (Na) and chlorine (Cl) could be detected. However, no traces of aluminum were found on the manufactured sheets (Figure 5).

Cell growth and differentiation on PCL/HA sheets

To investigate cell growth and adhesion on 75PCL25HA sheets, 50,000 eGFP-labeled SCP-1 cells were seeded per sheet (sheet geometry 1, see Figure 4) and cultivated statically in DMEM for 5 days. Cells growing on cell culture

dishes and on unprocessed PCL/HA were used as a control.

Cells adhered and grew homogeneously on the 75PCL25HA sheets (Figure 6(a)) as well as on unprocessed PCL/HA. The cell morphology was comparable to the cells growing on a cell culture dish (Figure 6(b) and (c)).

To investigate the cellular response of SCP-1 cells to differentiation factors, cells were cultivated in ODM for 21 days. Staining of calcium depositions in the extracellular matrix of mature osteoblasts was used to determine if the differentiation was successful.

In contrast to cells cultivated in DMEM (Figure 7(a)), the staining with ARS revealed high amounts of calcium depositions in the extracellular matrix of cells which were cultivated in ODM while growing on LC processed PCL/HA (Figure 7(b) and (c)) as well as on unprocessed PCL/HA and on cell culture dishes. The differentiation of SCP-1 cells to mature osteoblasts is thus possible with cells growing on 75PCL25HA sheets.

Cell growth on stacked PCL/HA scaffolds

To investigate cell growth on SSCs made of 50 circular 75PCL25HA sheets (Figure 4(b)), single sheets were seeded with 50,000 SCP-1 cells and cultivated in DMEM for 1 hour separately. Subsequently, the sheets were stacked with alternating orientation (Figure 2) to form an SSC with interconnecting pore structure and placed in an oxygen controlled perfusion microbioreactor to ensure a proper nutrient and oxygen supply of the 3DCC. The circular sheet shape was chosen for 3DCC, to facilitate a homogeneous nutrient and oxygen supply in the SSC.

SCP-1 cells were cultivated in the SSC for a minimum of 5 days. Subsequently, the distribution of the cells in the SSC was investigated. The distribution of cells throughout the scaffold was easily assessable by disassembling the SSC and analyzing the scaffold sheet by sheet. The SSC
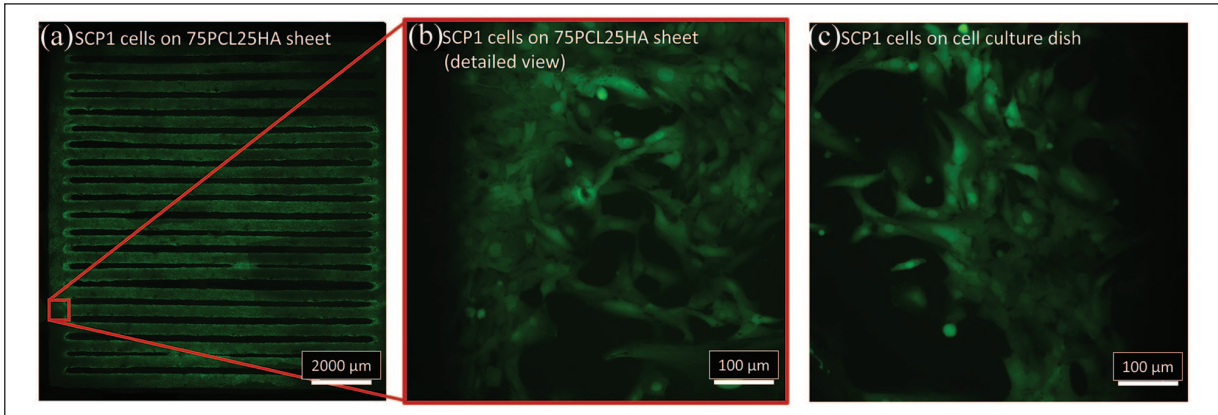
Figure 6. Fluorescence images showing growth and morphology of eGFP-labeled SCP1 cells on 75PCL25HA sheets, after 5 days of cultivation: (a) SCP-1 cell growing homogeneously on a 75PCL25HA sheet, stacked from 9 frames, 2.5× magnification; (b) SCP-1 cell morphology on 75PCL25HA sheet, GFP, 20× magnification; and (c) SCP-1 cell morphology on a cell culture dish, GFP, 20× magnification.
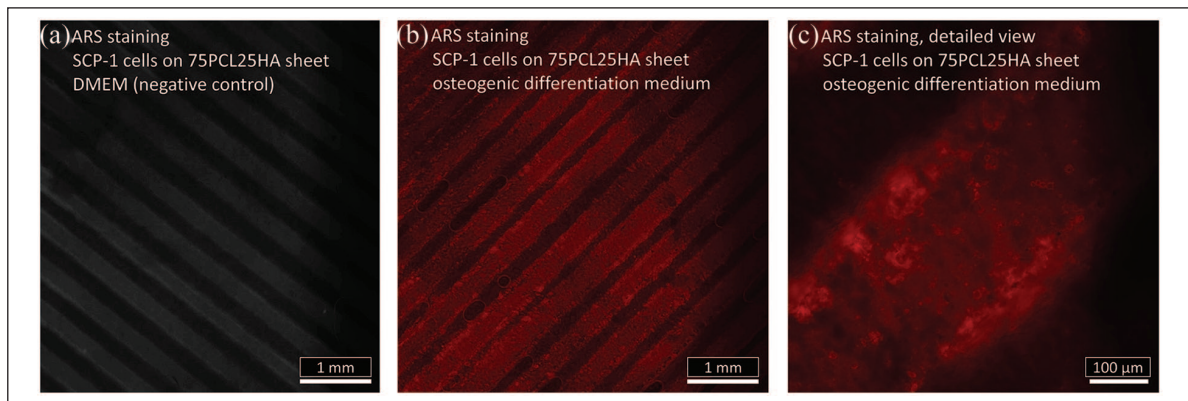

Figure 7. Investigation of differentiation of SCP-1 cells on PCL/HA sheets to osteoblasts after 21 days of cultivation, ARS-staining. Fluorescence images of Alizarin Red-S (ARS) stained SCP-1 cell cultures on 75PCL25HA sheets after 21 days of cultivation: (a) control, cultivation in DMEM, 2.5× magnification; (b) cultivation in ODM, 2.5× magnification; and (c) cultivation in ODM, 20× magnification.

was homogeneously overgrown, thus cells and sheets formed a coherent TE graft. The areas where the single sheets were in contact with each other were clearly visible in the fluorescence images of the SCP-1 cells (Figure 8).

Discussion

Generation of PCL/HA sheets

The generation of sheet-based scaffolds made of PCL/HA composite materials via LC was shown to be feasible. The developed method is easy to carry out, fast, and reproducible. Compared to other manufacturing methods, the sheet generation via LC does not require specific equipment but a standard commercially available LC device.

Prior to LC, a PCL/HA foil has to be created. For this purpose, an aluminum mold was used, since the great thermal conductivity of aluminum allows for both homogeneous

heating during the casting process and fast dissipation of the laser energy during the cutting process. Even though lasers operating in the kilowatt range are needed to cut aluminum,[29] it was investigated if traces of aluminum can be found on the cut edges of manufactured sheets. Therefore, SEM and EDX analyses were performed. Besides the main components of HA and PCL, platinum (sheets were sputtered with Pt prior to the measurement) and traces of sodium and chlorine (most likely transferred on the sheets during handling) were detected. Consequently, the use of an aluminum mold is unproblematic for the generation of the PCL/HA foil.

The LC process is suitable for PCL/HA ratios between 0% and 50% HA, which is comparable to other manufacturing methods like FDM, electrospinning and porogen leaching.[6,9,18,24,30,31] However, PCL/HA foils with 25% HA were found to have the best properties regarding processability and sheet stability. If lower quantities of HA are used, the processing of the composite material is
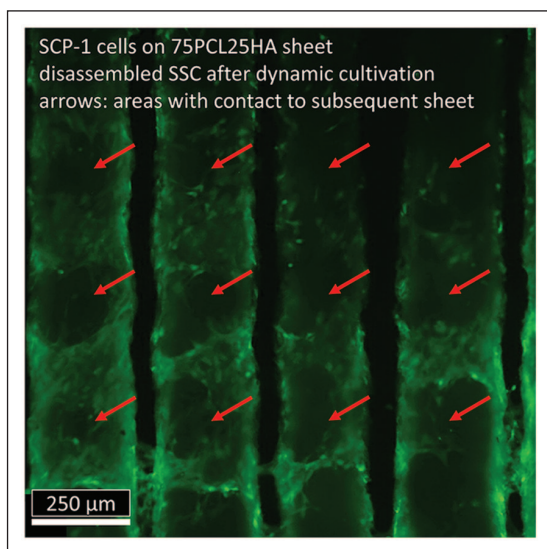
Figure 8. SCP-1 cells on a 75PCL25HA sheet after cultivation for 5 days as SSC in an oxygen controlled perfusion microbioreactor.
Fluorescence image (GFP) of SCP-1 cells growing on a 75PCL25HA sheet after cultivation of 5 days as SSC in an oxygen controlled microbioreactor and subsequent disassembling to single sheets. Areas, where single sheets were in contact with each other are indicated with red arrows, GFP, 10× magnification.

facilitated, but the resulting sheets are less stable and are damaged easily when they get removed from the aluminum mold. Also, the cut edges of manufactured sheets are not as smooth when lower HA quantities are used. The use of high HA quantities results in more stable sheets, but a less processable material, which impedes the creation of the PCL/HA foil.

The LC process itself is very robust and renders a well controllable manufacturing process, with variations between equally cut structures (e.g. diameters of circular structures) being lower than 20 μm. The design of different sheets is limited with respect to two structural features. First, structures between cut sections should be larger than 125 μm to be reliably stable and second, the width of the smallest possible section is about 40 μm (4.5 W laser power, designed section width 0 μm).

The energy input by the laser leads to material removal, which results in both larger sections and smaller gaps between sections, and thus in deviations between the designed cutting template and the resulting sheet. Naturally, higher laser powers result in higher material removal and thus in higher deviations of the resulting sheets to the CAD designed templates (Figure 3). Thus, lower laser powers are favorable for the manufacturing process.

Furthermore, the use of lower laser powers can lessen undesirable effects in the HAZ, like the alteration of the semi-crystalline structure of the processed polymer.[32] A higher crystallinity percentage can be observed in the HAZ

of polymers, which were processed at high laser powers. Naturally, these changes in crystallinity can have an effect on the degradation of the material.[33,34] Even though a relatively low laser power and a high laser head travel speed were applied in the developed manufacturing process, to minimize effects in the HAZ,[32] the effect of LC on the biodegradation of the manufactured sheets has to be further investigated.

The mechanical properties of 75PCL25HA sheets were investigated using a Mach1 mechanical tester. A YM of 110 ± 18 MPa and an UTS of 3.05 ± 0.80 MPa were calculated from tensile tests of five single sheets. These values are well in the expected range for PCL/HA composite materials.[35] However, these values only represent single sheets. If sheets are stacked to form a scaffold, the compression modulus should be determined, to investigate the shape-persistency and durability of the created scaffold. However, this value is not only dependent on the used material but also on the scaffold's architecture.[36,37] Consequently, the compressive modulus has to be investigated for each SSC design individually.

Compared to FDM printing, the LC process circumvents drawbacks like nozzle clogging and instability of subjacent layers during the printing process, while offering comparable flexibility and reproducibility. Furthermore, FDM printing requires slurries with exact viscosities, for proper printing,[18,21,22] which is not the case for the LC process, which therefore facilitates the production process substantially. Compared to other scaffold fabrication methods, pore interconnectivity—which can be problematic, for instance, for porogen leaching—is guaranteed, when sheets are stacked to a scaffold (SSC). In addition, the size of the SSC is not limited to smaller sizes, since there is no risk of residual solvents or porogens which could remain in larger scaffolds and hamper cell growth and viability (porogen leaching) or poor mechanical integrity (electrospinning).[22,38]

Cell growth and differentiation on PCL/HA sheets

Besides the physical properties like pore size and porosity, TE scaffolds have to allow cells to adhere, grow, and differentiate to form functional tissue. PCL/HA is known to be a highly functional composite material for bone TE applications.[9,39–41] However, LC is prone to generate a HAZ when thermoplastic materials are cut.[32] Beside the executed cut, the material in the HAZ can alter its properties due to heat exposure and subsequent cooling.[42,43] Consequently, we investigated the adherence and growth of hMSCs on the manufactured PCL/HA sheets and the differentiation potential of hMSCs when exposed to osteogenic differentiation factors.

The hMSC cell line SCP-1 was adhering and growing homogeneously on PCL/HA sheets, including HAZs,

while the cells maintained their typical morphology[27] (Figure 6). Furthermore, no differences in cell growth, adherence, or morphology were observed, when cells were cultivated on non-processed PCL/HA foil.

The testing of the differentiation potential of SCP-1 cells growing on the manufactured sheets was equally conclusive. Cells differentiated into osteoblasts within a cultivation period of 21 days in ODM, which was verified by staining calcium depositions in the extracellular matrix using ARS (Figure 7). The same results were found for SCP-1 cells growing on non-processed PCL/HA foil or cell culture dishes. Consequently, the processing via LC did not alter the properties of the material in a significant way with regard to cell growth, adherence, and cellular response to osteogenic differentiation factors. It has to be noted that calcium is a main component of HA. Thus, ARS could also stain exposed HA particles on the surface of the sheets,[44] possibly leading to false positive results. However, no staining was visible, if the sheets were fully overgrown with non-differentiated cells (Figure 7(a)).

Cell growth on stacked PCL/HA sheet scaffolds

Important properties of a functional scaffold are pore size, porosity, and the presence of an interconnecting pore network.[1,4,5] These parameters can be controlled precisely and reproducibly using the LC process. By stacking 50 circular sheets to an SSC, cylindrical scaffolds of 10 mm diameter and 10 mm height, with theoretical pore sizes of 300 μm, an interconnecting pore network, and porosities of 60% (approximated from the CAD model according to Loh and Choong[45]) can be created. It has to be considered that these porosity values can differ slightly from values obtained by, for instance, a gravimetric porosity determination.[46] However, scaffold and pore size, as well as the porosity, are variable and dependent on the initial sheet design.

The advantage of the SSC in contrast to solid scaffolds is the possibility to assemble and disassemble the scaffold. Thus, cell seeding and the investigation of cell fate after cultivation is considerably facilitated. However, single sheets can be welded together to form a solid scaffold structure, if desired.[6] On the contrary, the need to assemble the scaffold prior to cultivation can also be considered as a drawback of the SSC approach. The stacking of single sheets is time-consuming and the risk of contamination is higher when inoculated sheets are stacked to a 3D scaffold.

Prior cultivation, single sheets were inoculated with cells separately. Thus, the cell distribution could be assessed before the single sheets were stacked to a scaffold. Consequently, a homogeneous cell distribution is easier to achieve in the SSC. In contrast, solid scaffolds require complex dynamic cell seeding procedures to avoid inhomogeneous cell distributions and low initial cell densities.[14–16,47] To further speed up the cell seeding procedure, and to maximize seeding efficiencies on the PCL/HA sheets, the use of cell sheets[48,49] is recently under investigation. Cell sheets can be produced by using cell culture dishes with temperature responsive surfaces. As a result, PCL/HA sheets could be inoculated with contiguous, confluent cells with intact ECM prior assembly to an SSC.

After inoculation with SCP-1 cells and stacking to an SSC, the construct was cultivated for 5 days in an oxygen controlled perfusion bioreactor[28] to provide sufficient oxygen and nutrient supply. Subsequently, the SSC was disassembled and cell fate was analyzed. After a cultivation period of 5 days, the SSC was overgrown with cells and formed a coherent structure. The areas where the single sheets were in contact with each other were clearly visible in the fluorescence image of GFP-labeled cells (Figure 8). The possibility to disassemble the scaffold after cultivation is advantageous when homogeneity of, for instance, cell growth or differentiation has to be assessed. Compared to solid scaffolds, which would have to be cut prior analysis,[47,50] a much simpler workflow is possible using SSCs.

Laser-cut sheets could not only be used for the generation of SSCs but also for the generation of synergetic TECs by adding hydrogel layers in between laser-cut sheets, to provide both mechanical stability of the solid scaffold as well as the highly biomimetic environment of the hydrogel. Over recent years, different manufacturing techniques were used to develop different scaffold/hydrogel hybrid systems.[51–53] However, the feasibility of using laser-cut sheets for the generation of a hydrogel/scaffold hybrid system will be investigated in further studies.

Conclusion

A novel method for the generation of sheet-based scaffolds via LC has been introduced. The LC process is fast, reproducible, and highly flexible, and allows for the generation of sheets out of PCL/HA composite material in the range of 0%–50% HA. Single sheets can be stacked together to form a coherent scaffold structure with interconnecting pores. Cell adherence, growth, and osteogenic differentiation were shown to be feasible on the manufactured PCL/HA sheets. Calcium depositions were clearly present in the samples which were cultivated in ODM (Figure 6), indicating that the developed manufacturing method is suitable for the generation of functional PCL/HA scaffolds for TE applications. The use of SSCs can simplify both investigation of cell distribution after cultivation and cell seeding prior to cultivation. Also, the generation of scaffold/hydrogel hybrid systems, for instance, for vascularization approaches could be possible. Consequently, the generation of SSCs by LC offers new possibilities for TE research.

currently an employee of the Novartis Institutes of Biomedical Research, Basel, Switzerland.

Declaration of conflicting interests

The author(s) declared no potential conflicts of interest with respect to the research, authorship, and/or publication of this article.

Funding

References

1. Ikada Y. Challenges in tissue engineering. *J R Soc Interface* 2006; 3: 589–601.

2. Loh QL and Choong C. Three-dimensional scaffolds for tissue engineering applications: role of porosity and pore size. *Tissue Eng Part B Rev* 2013; 19(6): 485–502.

3. Mikos AG, Bao Y, Cima LG, et al. Preparation of poly(glycolic acid) bonded fiber structures for cell attachment and transplantation. *J Biomed Mater Res* 1993; 27(2): 183–189.

4. Hutmacher DW. Scaffolds in tissue engineering bone and cartilage. *Biomater* 2000; 21: 2529–2543.

5. An J, Teoh JEM, Suntornnond R, et al. Design and 3D printing of scaffolds and tissues. *Engineering* 2015; 1: 261–268

6. He F-L, Li D-W, He J, et al. A novel layer-structured scaffold with large pore sizes suitable for 3D cell culture prepared by near-field electrospinning. *Mat Sci Eng C* 2017; 86: 18–27.

7. Naughton GK, Tolbert WR and Grillot TM. Emerging developments in tissue engineering and cell technology. *Tissue Eng* 1995; 1(2): 211–219.

8. Badylak SF and Gilbert TW. Immune response to biologic scaffold materials. *Semin Immunol* 2008; 20(2): 109–116.

9. Chuenjitkuntaworn B, Inrung W, Damrongsri D, et al. Polycaprolactone/hydroxyapatite composite scaffolds: preparation, characterization, and in vitro and in vivo biological responses of human primary bone cells. *J Biomed Mater Res A* 2010; 94(1): 241–251.

10. Do A-V, Smith R, Acri TM, et al. 3D printing technologies for 3D scaffold engineering. In: Deng Y and Kuiper J (eds) *Functional 3D tissue engineering scaffolds: materials, technologies and applications*. Amsterdam: Elsevier Ltd., 2018, pp. 203–234.

11. Wutticharonemongkol P, Sachavanakit N, Pavasant P, et al. Novel bone scaffolds of electrospun polycaprolactone fibers filled with nanoparticles. *J Nanosci Nanotechnol* 2006; 6: 514–522.

12. Shikinami Y and Okuno M. Bioresorbable devices made of forged composites of hydroxyapatite (HA) particles and poly-L-lactide (PLLA): part I. Basic characteristics. *Biomaterials* 1998; 20: 859–877.

13. Roseti L, Parisi V, Petretta M, et al. Scaffolds for bone tissue engineering: state of the art and new perspectives. *Mater Sci Eng C Mater Biol Appl* 2017; 78: 1246–1262.

14. Vunjak-Novakovic G, Obradovic B, Martin I, et al. Dynamic cell seeding of polymer scaffolds for cartilage tissue engineering. *Biotechnol Prog* 1998; 14(2): 193–202.

15. Melchels FP, Barradas AM, vanBlitterswijk CA, et al. Effects of the architecture of tissue engineering scaffolds on cell seeding and culturing. *Acta Biomater* 2010; 6(11): 4208–4217.

16. Alvarez-Barreto JF, Linehan SM, Shambaugh RL, et al. Flow perfusion improves seeding of tissue engineering scaffolds with different architectures. *Ann Biomed Eng* 2007; 35(3): 429–442.

17. Suntornnod R, An J, Yeong WY, et al. Hybrid membrane based structure: a novel approach for tissue engineering scaffold. In: *ICAM-BM 2014*, Beijing, China, 13 November. Beijing: ICAM-BM, 2014, pp. 41–42.

18. Goncalves EM, Oliveira FJ, Silva RF, et al. Three-dimensional printed PCL-hydroxyapatite scaffolds filled with CNTs for bone cell growth stimulation. *J Biomed Mater Res B Appl Biomater* 2016; 104(6): 1210–1219.

19. Zhao P, Haibing GU, Mi H, et al. Fabrication of scaffolds in tissue engineering: a review. *Front Mech Eng* 2018; 13: 107–119.

20. Temple JP, Hutton DL, Hung BP, et al. Engineering anatomically shaped vascularized bone grafts with hASCs and 3D-printed scaffolds. *J Biomed Mater Res A* 2014; 102: 1–9.

21. Wang X, Jiang M, Zhou Z, et al. 3D printing of polymer matrix composites: a review and prospective. *Composites Part B* 2016; 110: 442–458.

22. Trachtenberg JE, Kasper FK and Mikos AG. Polymer Scaffold fabrication. In: Lanza R, Langer R and Vacanti J (eds) *Principles of tissue engineering*. 4th ed. Burlington, MA: Academic Press, 2014, pp. 423–440.

23. Khorshidi Solouk A, Mirzadeh H, Mazinani S, et al. A review of key challenges of electrospun scaffolds for tissue-engineering applications. *J Tissue Eng Regen Med* 2016; 10(9): 715–738.

24. Tan Q, Li S, Ren J, et al. Fabrication of porous scaffolds with a controllable microstructure and mechanical properties by porogen fusion technique. *Int J Mol Sci* 2011; 12(2): 890–904.

25. Todd RH, Allen DK and Alting L. *Manufacturing processes reference guide*. South Norwalk, CT: Industrial Press Inc, 1994.

26. Caristan CL. *Laser cutting guide for manufacturing*. Dearborn, MI: Society of Manufacturing Engineers, 2004.

27. Bocker W, Yin Z, Drosse I, et al. Introducing a single cell-derived human mesenchymal stem cell line expressing hTERT after lentiviral gene transfer. *J Cell Mol Med* 2008; 12(4): 1347–1359.

28. Schmid J, Schwarz S, Meier-Staude R, et al. A perfusion bioreactor system for cell seeding and oxygen-controlled cultivation of tree-dimensional cell cultures. *Tissue Eng Part C Methods* 2018; 24: 585–595.

29. Stournaras A, Stavropoulos P, Salonitis K, et al. An investigation of quality in CO_2 laser cutting of aluminum. *CIRP J Manuf Sci Technol* 2009; 2: 61–69.

30. D'Amora U, D'Este M, Eglin D, et al. Collagen density gradient on 3D printed poly(e-caprolactone) scaffolds for interface tissue engineering. *J Tissue Eng Regen Med* 2018; 12: 321–329.

31. Wang Y, Liu L and Guo S. Characterization of biodegradable and cytocompatible nano-hydroxyapatite/polycaprolactone porous scaffolds in degradation in vitro. *Polym Degrad Stab* 2010; 95: 207–213.

32. Tamrin KF, Nukman Y, Choudhury LA, et al. Multiple-objective optimization in precision laser cutting of different thermoplastics. *Opt Lasers Eng* 2015; 67: 57–65.

33. Guerra AJ, Farjas J and Ciurana J. Fibre laser cutting of polycaprolactone sheet for stents manufacturing: a feasibility study. *Opt Laser Technol* 2017; 95: 113–123.

34. Passaglia E, Bertoldo M, Coiai S, et al. The effect of crystalline morphology on the degradation of polycaprolactone in a solution of phosphate buffer and lipase. *Polym Adv Technol* 2008; 19: 1901–1906.

35. Baji A, Wong SC and Srivatsan TS. Processing methodologies for polycaprolactone-hydroxyapatite composites: a review. *Mater Manuf Process* 2006; 21: 211–218.

36. Sabree I, Gough JE and Derby B. Mechanical properties of porous ceramic scaffolds: influence of internal dimensions. *Ceramics Int* 2015; 41: 8425–8432.

37. Shor L, Güçeri S, Wen X, et al. Fabrication of three-dimensional polycaprolactone/hydroxyapatite tissue scaffolds and osteoblast-scaffold interactions in vivo. *Biomaterials* 2007; 28: 5291–5297.

38. Murphy MB and Mikos AG. Polymer scaffold fabrication. In: Lanza R, Langer R and Vacanti J (eds) *Principles of tissue engineering*. 3rd ed. Burlington, MA: Academic Press, 2007, pp. 309–322.

39. Hutmacher DW, Schantz T, Zein I, et al. Mechanical properties and cell cultural response of polycaprolactone scaffolds designed and fabricated via fused deposition modeling. *J Biomed Mater Res* 2001; 55(2): 203–216.

40. Chuenjitkunataworn B, Osathanon T, Nowwarote N, et al. The efficacy of polycaprolactone/hydroxyapatite scaffold in combination with mesenchymal stem cells for bone tissue engineering. *J Biomed Mater Res Part A* 2015; 104: 264–271.

41. D'Anto V, Raucci MG, Guarino V, et al. Behaviour of human mesenchymal stem cells on chemically synthesized HA-PCL scaffolds for hard tissue regeneration. *J Tissue Eng Regen Med* 2016; 10(2): E147–E154.

42. Choudhury IA and Shirley S. Laser cutting of polymeric materials: An experimental investigation. *Opt Laser Technol* 2010; 42: 503–508.

43. Davim JP, Barricas N, Conceicao M, et al. Some experimental studies on CO_2 laser cutting quality of polymeric materials. *J Mater Proc Technol* 2008; 198: 99–104.

44. Moriguchi T, Yano K, Nakagawa S, et al. Elucidation of adsorption mechanism of bone-staining agent alizarin red S on hydroxyapatite by FT-IR microspectroscopy. *J Colloid Interface Sci* 2003; 260(1): 19–25.

45. Loh QL and Choong C. Three-dimensional scaffolds for tissue engineering applications: role of porosity and pore size. *Tissue Eng Part B Rev* 2013; 19(6): 485–502.

46. Lee KW, Wang S, Lu L, et al. Fabrication and characterization of poly(propylene fumarate) scaffolds with controlled pore structures using 3-dimensional printing and injection molding. *Tissue Eng* 2006; 12(10): 2801–2811.

47. Wendt D, Marsano A, Jakob M, et al. Oscillating perfusion of cell suspensions through three-dimensional scaffolds enhances cell seeding efficiency and uniformity. *Biotechnol Bioeng* 2003; 84(2): 205–214.

48. Yamato M and Okano T. Cell sheet engineering. *Mater Today* 2004; 7: 42–47.

49. Valmikinathan CM, Chang W, Xu J, et al. Self-assembled temperature responsive surfaces for generation of cell patches for bone tissue engineering. *Biofabrication* 2012; 4: 035006.

50. Thevenot P, Nair A, Dey J, et al. Method to analyze three-dimensional cell distribution and infiltration in degradable scaffolds. *Tissue Eng Part C Methods* 2008; 14(4): 319–331.

51. Ovsianikov A, Khademhosseini A and Mironov V. The synergy of scaffold-based and scaffold-free tissue engineering strategies. *Trends Biotechnol* 2018; 36(4): 348–357.

52. Shim JH, Kim JY, Park M, et al. Development of a hybrid scaffold with synthetic biomaterials and hydrogel using solid freeform fabrication technology. *Biofabrication* 2011; 3(3): 034102–034109.

53. Igwe JC, Mikael PE and Nukavarapu SP. Design, fabrication and in vitro evaluation of a novel polymer-hydrogel hybrid scaffold for bone tissue engineering. *J Tissue Eng Regen Med* 2014; 8(2): 131–142.